Models and measurements on the ALLEGRO PCB prototype designed at IJCLab

Ronic Chiche, Daniel Fournier, Nicolas Morange

Laboratoire de Physique des 2 infinis Irène Joliot-Curie

Bât. 100, 15 rue Georges Clémenceau, 91405 Orsay cedex

UMR9012 – CNRS / Université Paris-Saclay / Université Paris Cité

Models and measurements on the ALLEGRO PCB prototype designed at IJCLab

Authors: Ronic Chiche, Daniel Fournier, Nicolas Morange (IJCLab)

22 January 2025

Abstract

A prototype multilayer printed circuit board, featuring the main characteristics necessary for a high granularity liquid argon sampling calorimeter, has been produced and tested for signal propagation. The board, of size limited to 3 adjacent towers, corresponds otherwise to the FCC-ee Allegro barrel detector concept.

When injecting a triangular signal, direct and crosstalk signals, filtered numerically with a range of shaping times between 20 ns and 200 ns, have been recorded and successfully compared to simulations.

Introduction

In the Allegro experiment foreseen for the future proposed FCC-ee collider at CERN, the electromagnetic calorimeter is a sampling calorimeter with noble liquid as active medium [1]. The central part is divided in two half-barrels housed in the same cryostat. Each half-barrel consists of 1536 slanted absorbers about 3 meters long, with the same number of interleaved electrode planes. The electrode planes are made of an assembly of several Printed Circuit Boards (PCB), of maximal size dictated by industrial standards (see Figure 1).

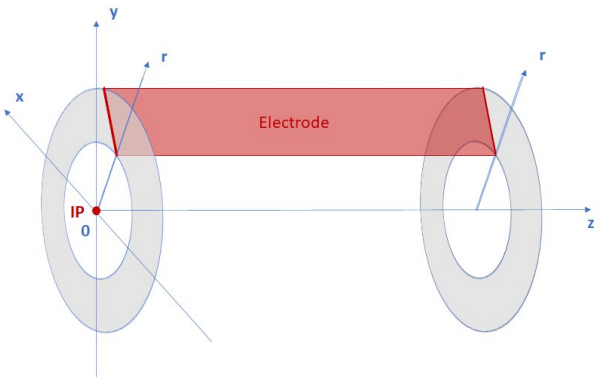

Figure 1: Schematics of a half-barrel, with the associated axis systems

Corresponding author : ronic.chiche@ijclab.in2p3.fr

The electrodes (see figure 2) are designed to projectively sample the showers produced by electrons or photons emitted at the interaction point (IP) as they travel through the calorimeter. Sampling the showers along theta requires dividing the electrode into towers, and sampling along the radial direction translates into division of the towers into cells. The closest (first) cell from the IP is the presampler (PS); the second cell is divided into four strips and is followed by ten other cells. An alternative scheme is also considered in which there are two cells before the strip section, but it is not studied in this work.

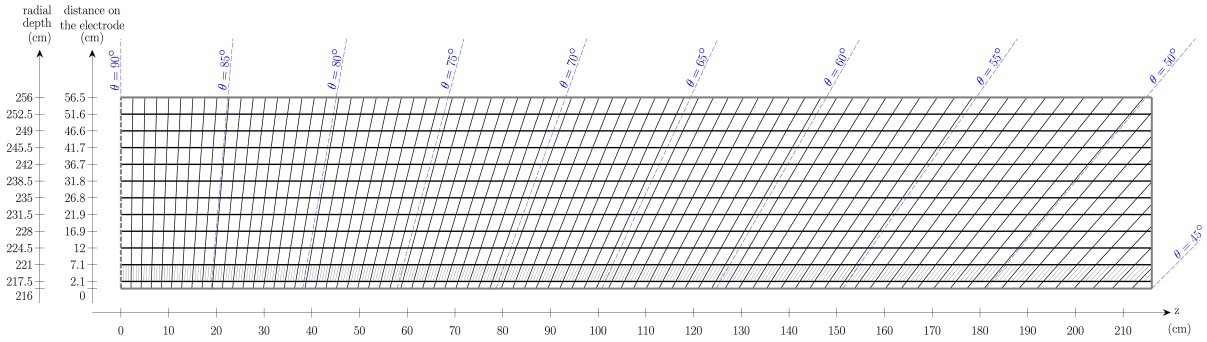

Figure 2: Main dimensions of an electrode plane

All the 15 signals coming from the PS, the four strips, and the ten other cells are routed using shielded striplines inside the PCB, to the back of the electrode, where a connector allows to route the signals from each tower to readout electronics.

Each cell is a sandwich of several layers in the thickness of the PCB (see Figure 3):

- The signal layer on which the signal will travel from the cell to the connector
- The shielding layer, just above and below the signal layer to minimize the spread of the induced electromagnetic field. Imperfect shielding results in capacitive crosstalk with neighboring pads or signal lines.
- The pad layer, which will collect the induced ionized charges
- The High Voltage (HV) layer which produces the electric field between the electrodes and the absorbers, at ground voltage.

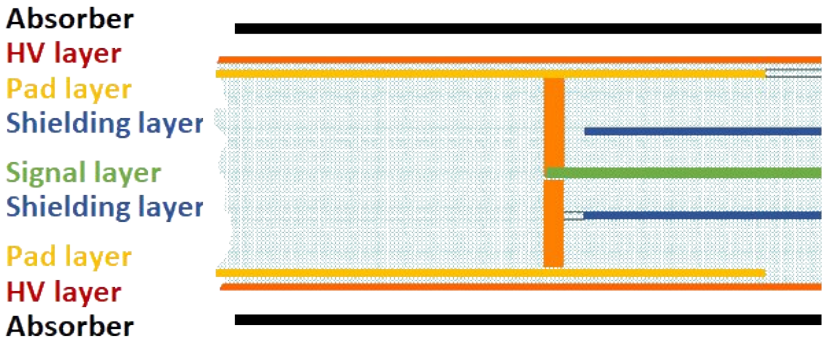

Figure 3: Transverse view of a PCB showing the 7 conductive layers

The electrodes are separated from each other by dense absorber plates (to create particle showers in the detector) made of metal connected to the ground. Part of the current resulting from the drift of charged particles of the shower in the noble liquid will flow back to the cells through the absorber plates, the other part through the shielding layers.

This note describes the measurements and models of a prototype of a PCB, which is close to the reference PCB described above and was developed at IJCLab.

Design of the IJCLab PCB prototype

The prototype has been designed to be as close as possible to the reference design described above, without the complexity of the (pointing) real electrode geometry, which should not change the important electronic parameters, namely cell capacitance, stripline parameters, and channels cross-talk.

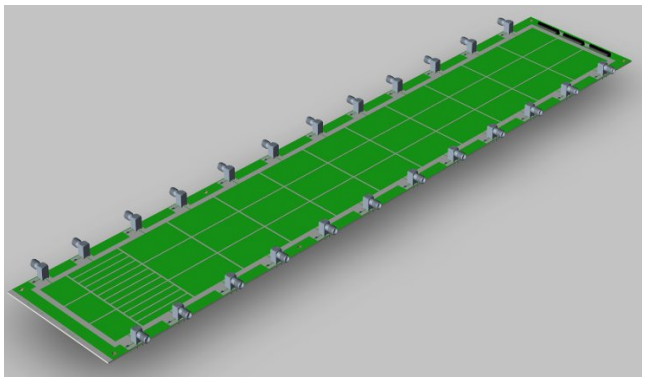

Figure 4: IJCLab PCB top view, with 3 towers of 15 channels

The PCB is 60 cm long, with three towers with a width of 3 cm. Each cell is 3x5 cm, except the PS, which is half-length (3x2.5 cm), and the four strips, which are 0.75x5 cm. SMA connectors with the signal pins connected to the pads were added on the sides of the PCB. Because their grounding is connected to the general ground of the board around the three towers and not directly to the striplines shielding, using them as input port produces an electromagnetic field all over the board, which induces large crosstalk signals. Thus, they were not used for the measurements presented in this note.

The reference design PCB described in the introduction has seven layers of metal, which is impossible to produce symmetrically with a stack of laminated insulators and impregnated fiber layers (pre-preg). Then, we decided to double the signal layer to get a perfectly symmetric structure.

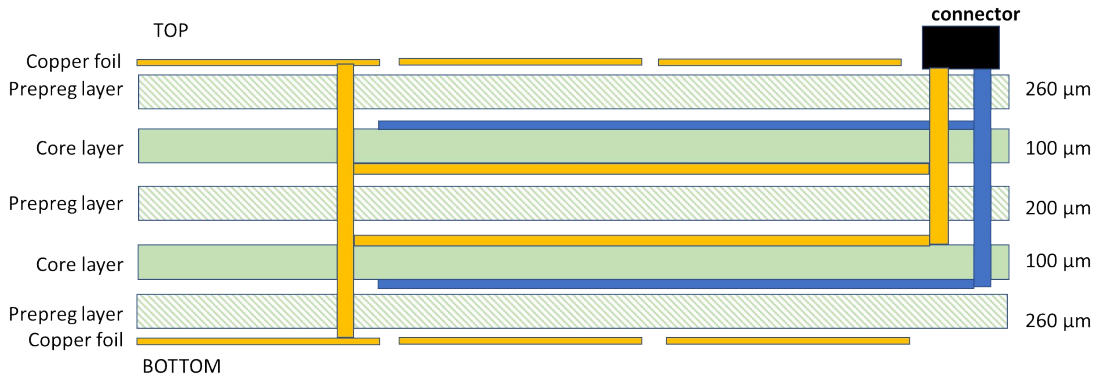

Figure 5: IJCLab PCB side view with pads on top and bottom and the double stripline in the middle

The aim of the HV layer, very close to the pad layer, is to produce an electric field between the top and bottom of each cell, being connected to each pad through a high-capacitance (low-impedance) element. This layer should not play an important role in the signal and crosstalk behavior as the HV-

pad capacitance is very large compared to the pad-shield capacitance, and the layer is at a floating potential. We decided not to integrate this layer into the present design.

All the three towers have the same general trace routing from pads to the end connector, to maximize the distance between the striplines: see figure 6.

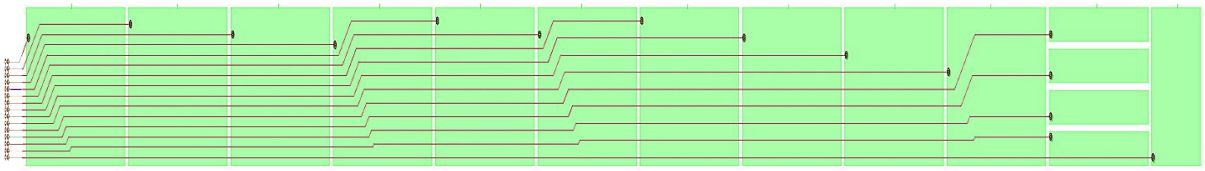

Figure 6: Striplines routing for the 3rd PCB tower without additional shielding (1st and 2nd towers have similar routing and additional lateral shielding as shown in figure 7))

The first and second towers have additional lateral shieldings:

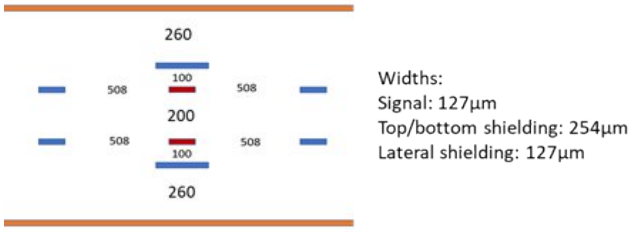

Figure 7: Front view of the PCB's 1st and 2nd towers with lateral shieldings. Insulator thicknesses and signal and shielding widths are reminded.

The third tower has only top and bottom shieldings:

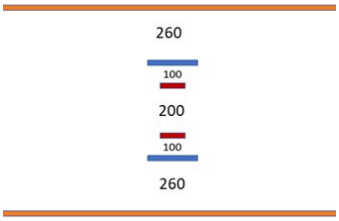

Figure 8: Front view of the pads, stripline with top/bottom shielding of the 3rd tower

The differential striplines model

The present stripline topology, where the same signal is transmitted over two different conductors, is the well-known differential stripline structure used in the common mode.

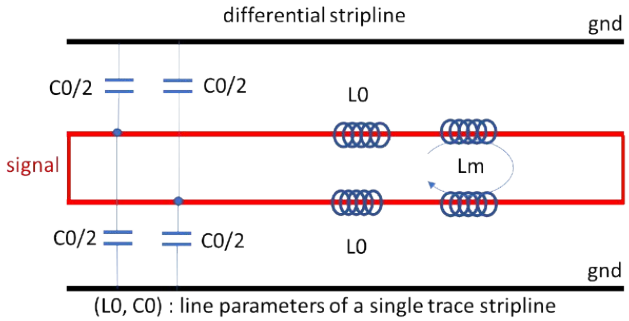

Figure 9: Differential stripline model with a double conductor for transporting the signal

If L_0 and C_0 are the equivalent self-inductance and capacitance of the single conductor stripline, one can express the elements of the double conductor stripline used in common mode where L_m is the mutual inductance due to the loop formed by the two conductors:

$$\begin{cases} C_{diff} = 2C_0 \\ L_{diff} = \dfrac{L_0 + L_m}{2} \end{cases}$$

Equation 1: shows clearly that the capacitance of the line in the differential striplines model is twice what it would be with a single strip line. This is a clear disadvantage in terms of noise of this configuration, since series noise is at first order proportional to the (total) capacitance of the readout cell

With the present geometrical configuration of the single conductor, which is at 100µm and 300µm from the top and bottom grounds (https://www.elektroda.com/calculators/pcb-impedance-calculator-asymmetric-stripline) the following values are obtained¶

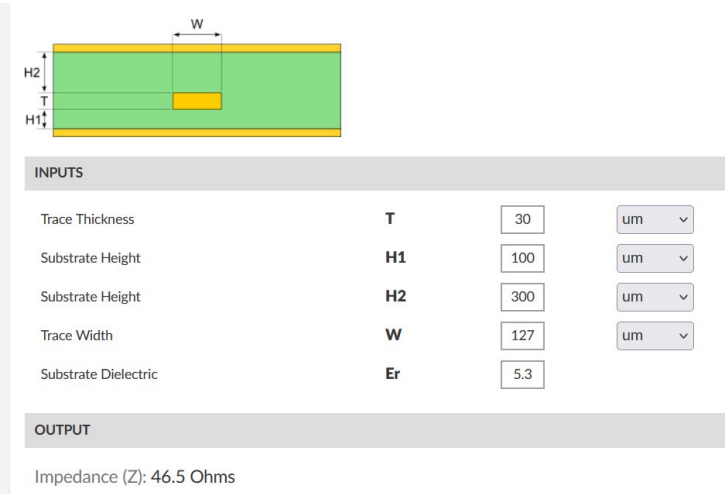

Figure 10: Electrokoda webpage capture resulting in 46.5 ohms characteristic impedance

$$\left.\begin{aligned} Z_{C0} &= \sqrt{\frac{L_0}{C_0}} \simeq 46.5\Omega \\ \sqrt{\varepsilon_r} &= c\sqrt{L_0 C_0} \simeq \sqrt{5.3} \end{aligned}\right\} \Rightarrow \begin{cases} C_0 = \dfrac{\sqrt{\varepsilon_r}}{cZ_{C0}} \simeq 165\,pF/m \\ L_0 = \dfrac{Z_{C0}\sqrt{\varepsilon_r}}{c} \simeq 357\,nH/m \end{cases}$$

Equation 2

Capacitance, speed, and characteristic impedance measurements

Capacitance measurements were done with a capacitance meter and with the rise time technique in response to a step. The capacitances measured in this way do not include the capacitance from pad to absorber. Given the gap width (between 1 and 2 mm), this missing part is expected to be small compared to the measured one.

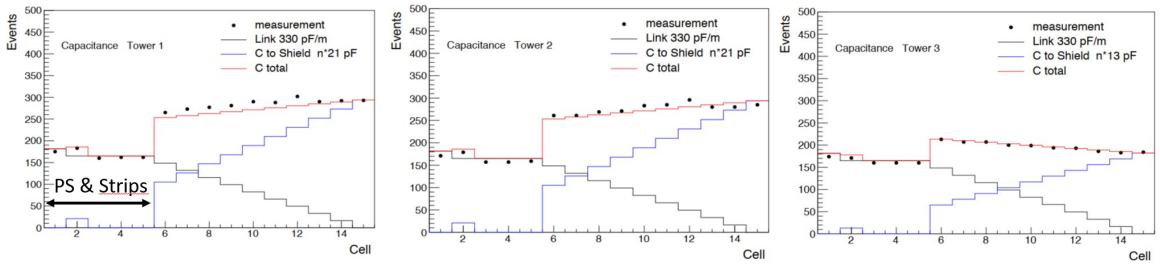

Figure 11: Total capacitance measurement for the 3 towers of the PCB with a fit of the lineic and pad-shielding parts. n is the number of signal lines (and ground shields) under a given pad.

A fit of the data exhibits a lineic capacitance of 330pF/m for the stripline in each of the three towers and an additional pad-ground capacitance proportional to the number (n) of ground shield strips below each pad.

The lineic capacitance values of the differential striplines agree with the prediction of the differential striplines model described above: $C_{diff} = 2C_0 = 330$ pF/m.

The pad-shield capacitance is 13pF/strip for the tower without lateral shielding, and 21pF/strip for the towers with lateral shielding.

A speed measurement was done on the longest stripline, using a voltage step to measure the duration of the voltage stair response: 5.4 ns for 56 cm, equivalent to an inverse speed of 9.6 ns/m. The height of the stair is also related to the characteristic impedance of the line, measured to be $Z_{c,diff} = 29\Omega$.

$$\left.\begin{aligned} C_0 &\simeq 165\,pF/m \\ L_0 &\simeq 357\,nH/m \\ L_m &\simeq 201\,nH/m \\ Z_{c0} &\simeq 46.5\,\Omega \end{aligned}\right\} \Rightarrow \left\{\begin{aligned} C_{diff} &= 2C_0 \simeq 330\,pF/m \\ L_{diff} &= \frac{L_0 + L_m}{2} \simeq 279\,nH/m \end{aligned}\right\} \Rightarrow \left\{\begin{aligned} Z_{c,diff} &= \frac{1}{2}\sqrt{\frac{L_0 + L_m}{C_0}} \simeq 29\Omega \\ v^{-1} &= \sqrt{(L_0 + L_m)C_0} \simeq 9.6\,ns/m \end{aligned}\right.$$

Equation 3

Adding a mutual inductance of about 200nH/m allows to obtain from the single conductor simulation the exact values of the differential stripline measurements (lineic capacitance, inverse speed and characteristic impedance).

Crosstalk capacitance measurements

The crosstalk performance of the PCB is directly related to the crosstalk elements between each pair of channels. Up to relatively high frequency, the capacitive crosstalk is the dominant term. Tthe crosstalk capacitances have been measured manually with a capacitance-meter used in differential mode. For that measurement, one has to nullify the voltage across one of the stray capacitances in order to measure a current (I_L) at the lower point which is the same as the one flowing across the crosstalk capacitance.

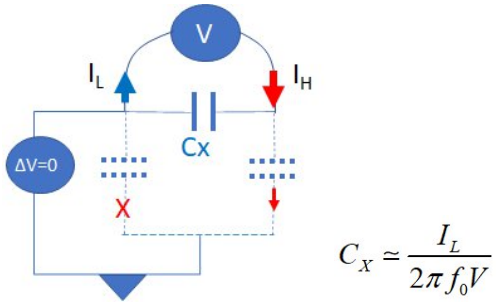

Figure 12: Crosstalk capacitance Cx measurement principle. Cx is surrounded by two stray capacitances in dashed lines. It is needed to cancel the voltage between the ground and the low voltage point, so that the current I_L is identical to the current across the capacitance.

The measured crosstalk capacitance values are in between 0.5pF and 5pF with the largest values between the closest neighbors (see Figure 13).

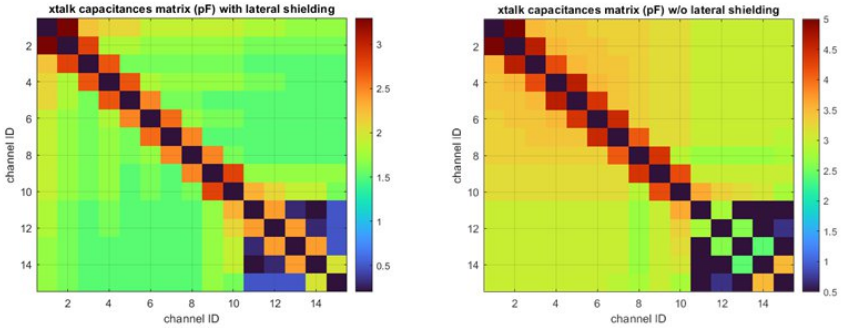

Figure 13: Crosstalk capacitances (in pF) for towers with lateral shielding (left) and for the 3rd tower without lateral shielding (right)

At first order, the crosstalk capacitances have two main components. One is the capacitance between a pad and the strip of another cell running below it, imperfectly shielded by the ground shields. The second one is the capacitance between two neighboring pads. The two components can be seen clearly on Figure 13. The largest capacitances are between neighboring channels in the radial direction, where both components apply. The channels 11-15 are related to the 4 strips and the presampler and have very few (0 or 1) striplines (see figure 6) below their pads and thus, a much lower crosstalk capacitance. The strips (11-14) have a neighboring pad-pad capacitance among themselves, along with a small pad-pad capacitance with cell 10 and cell 15.

Crosstalk signals measurement setup

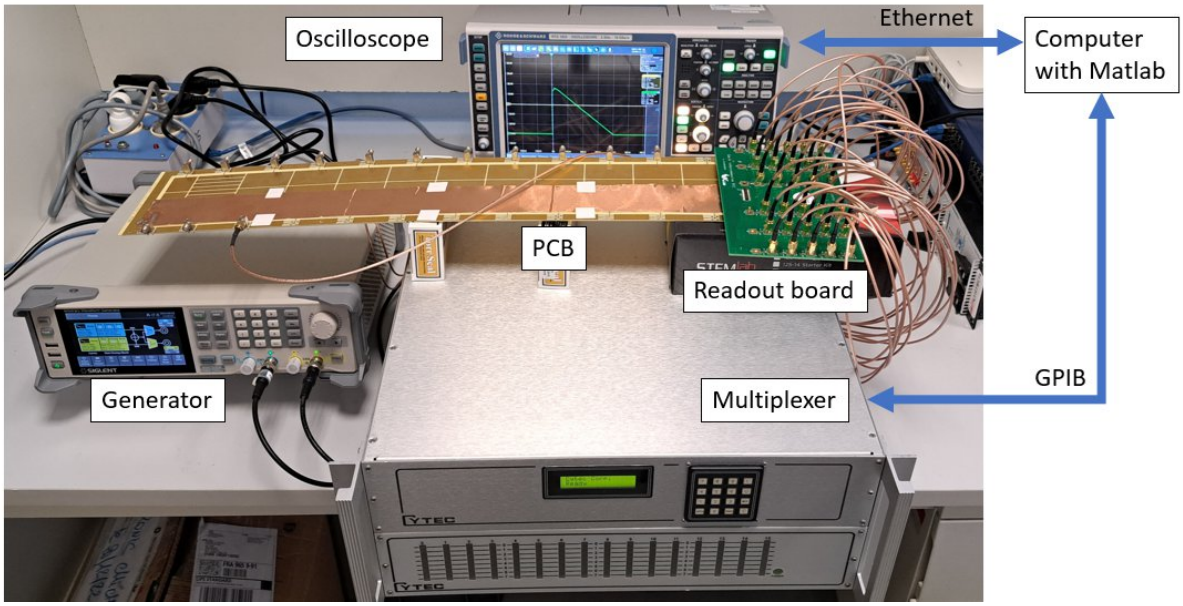

We present here the crosstalk signals measurement setup for which a readout board has been designed in order to access all the channels of a tower through its dedicated connector. As we need to send one signal to any channel of the PCB and to read all channels of the PCB with one channel of the oscilloscope, we used a multiplexer crate which embeds enough switches for the input signal, the direct signal output and the crosstalk signals measurement. For automation purposes, the oscilloscope is controlled via Ethernet and the multiplexer via GPIB by a Matlab script. Signal shaping, corresponding to a CR-RC2 filter with time constants ranging from 10 ns to 500 ns is applied numerically.

The signal propagation in this measurement setup is different from what it will be in the physics experiment: here the signal is injected from the readout connector, while it will be applied on the pad structure. We estimated the expected differences on the direct and cross-talk signal in these two cases using simulations.

Figure 14 presents the simulated setups: the physics signal case uses a current source on the pad, while the measurement system uses a voltage source applied on the readout end of the stripline.

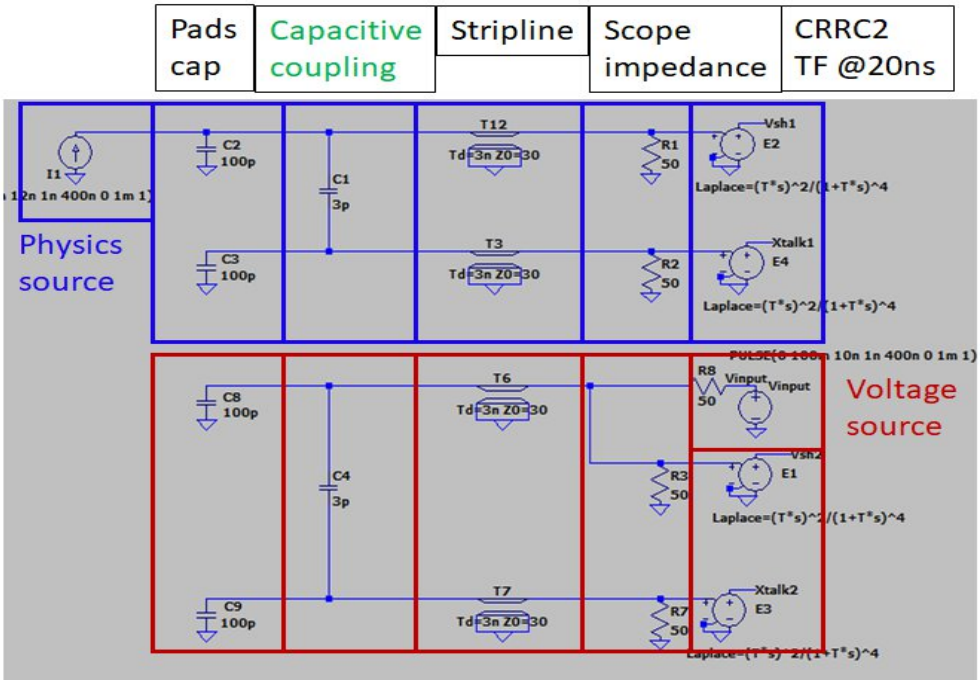

Figure 14: Simulation scheme using LTspice, to compare crosstalk signal with capacitive coupling with a physics or a generator source. Vsh is the direct measurement of the signal after 20ns shaping time and Xtalk is the crosstalk signal measurement.

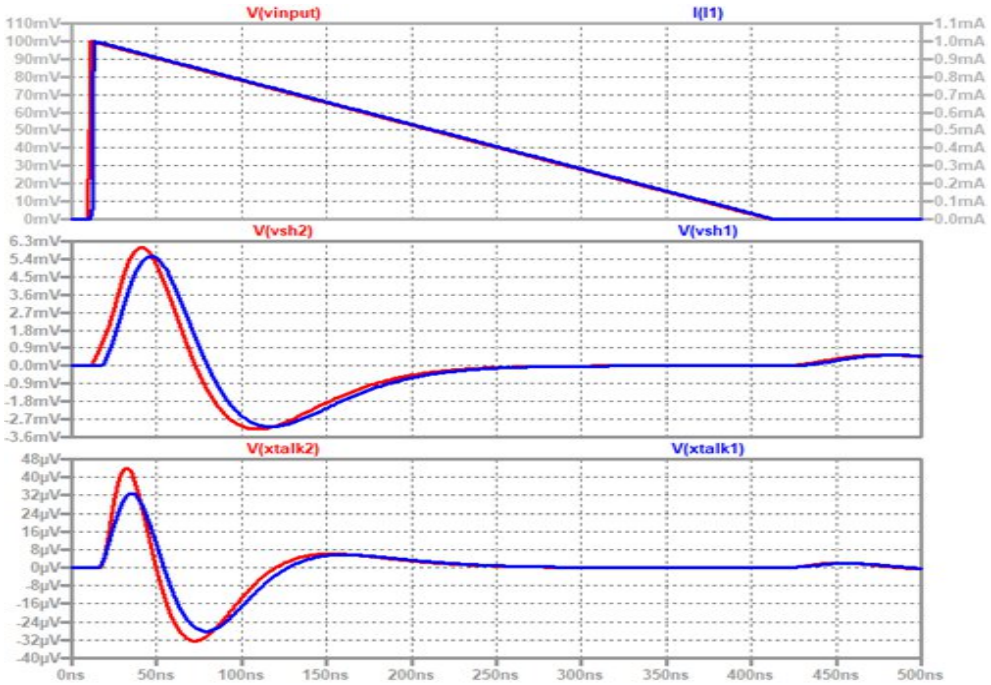

Figure 15: From simulation, comparison plots for direct and crosstalk signals for capacitive crosstalk. Vsh is the direct signal after 20ns shaping time and Xtalk is the crosstalk signal. Blue curves are for the physics simulation and red curves for the voltage source simulation.

For a capacitive crosstalk, figure 15 exhibits very similar simulated signals after shaping in amplitude and duration if one applies a physics source at the pad position (blue curve) or if one applies a generator source from the readout connector (red curve), both for the direct signal (Vsh, middle pane) or for the cross-talk signal (Xtalk, bottom pane).

One can do the same simulation for an inductive crosstalk:

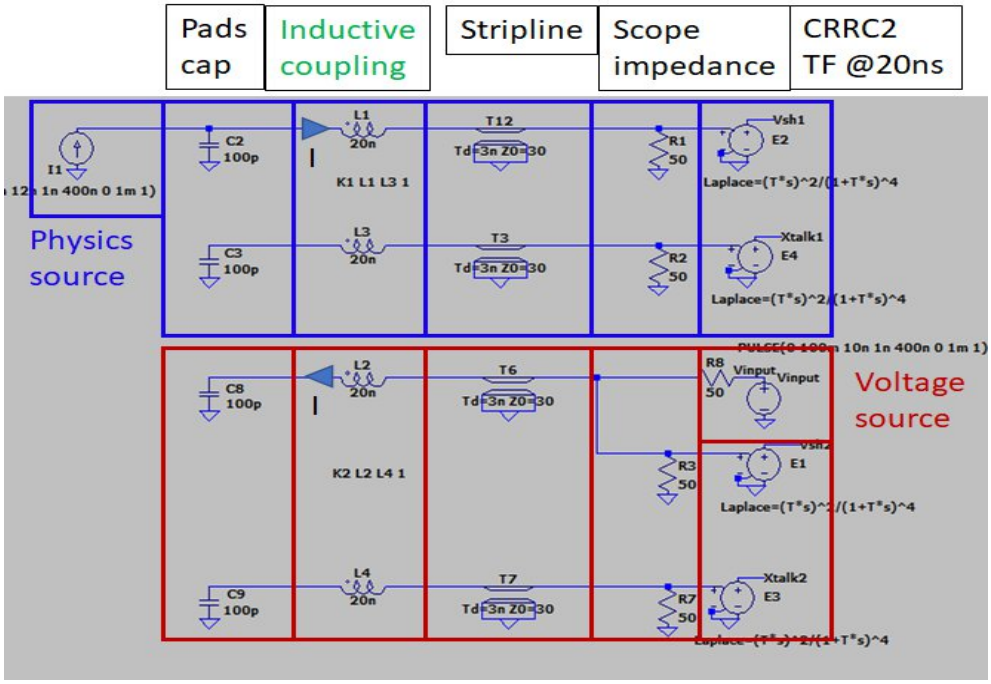

Figure 16: Simulation scheme using LTspice, to compare crosstalk signal with inductive coupling with a physics or a generator source . Vsh is the direct signal and Xtalk is the crosstalk signal.

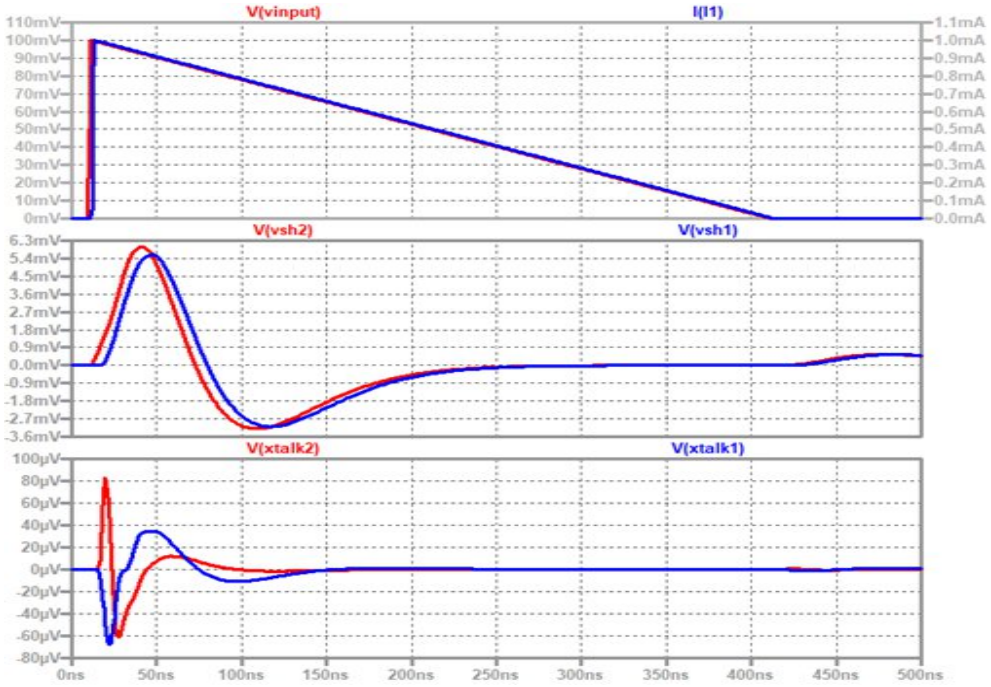

Figure 17: From simulation, comparison plots for direct and crosstalk signals for inductive crosstalk. Vsh is the direct signal after 20ns shaping time and Xtalk is the crosstalk signal. Blue curves are for the physics simulation and red curves for the voltage source simulation.

If one compares the simulations with an inductive crosstalk figure 17 exhibits similar direct signals after shaping (Vsh) in amplitude and duration if one applies a physics source at the pad position (blue curve) or if one applies a generator source from the readout connector (red curve). But the crosstalk signals are different. The peak values are similar but the sign is reverted because of the signs of the

source currents, symbolized by an arrow on figure 16. As a consequence, the ratio of the peak of the crosstalk to the peak of the direct signal is correctly estimated when injecting the signal from the readout connector. However the crosstalk when evaluated at the peak of the direct signal should be considered carefully because of the shape difference that should be taken into account: the measurement with a voltage source is almost zero while the real crosstalk from the physics signal is clearly much more important. For a longer shaping time the situation is possibly different (see below).

If one mixes inductive and capacitive coupling together for the generator source case, the crosstalk signal exhibits a specific shape with a double bump before the signal decay time:

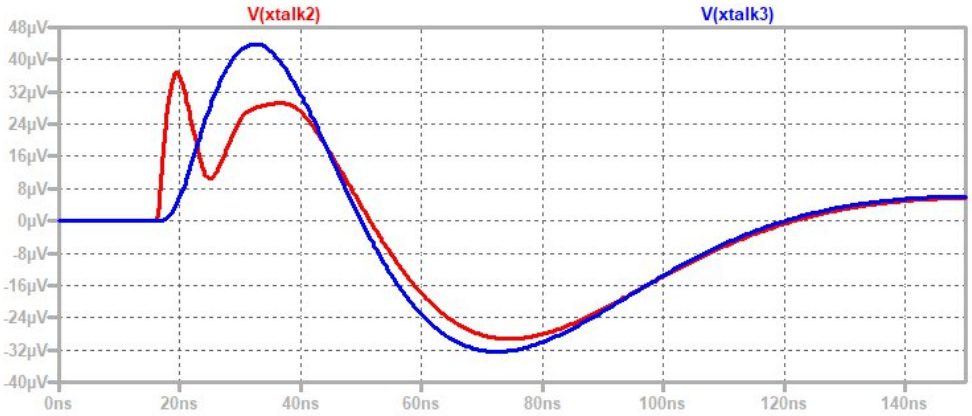

Figure 18: Typical simulated crosstalk signal with capacitive coupling only (blue curve) and with both capacitive and inductive coupling (red curve)

Crosstalk signals measurements

In this paragraph, we present in figures 19 and 20 the different crosstalk measurements done on tower 3 (without additional shielding) with the setup already described, with a shaping time of 20ns. The normalization of crosstalk signals correspond to a direct signal of 1V after shaping. This setup allows to show all crosstalk waveforms, relative to different cell injection and cell measurement configurations.

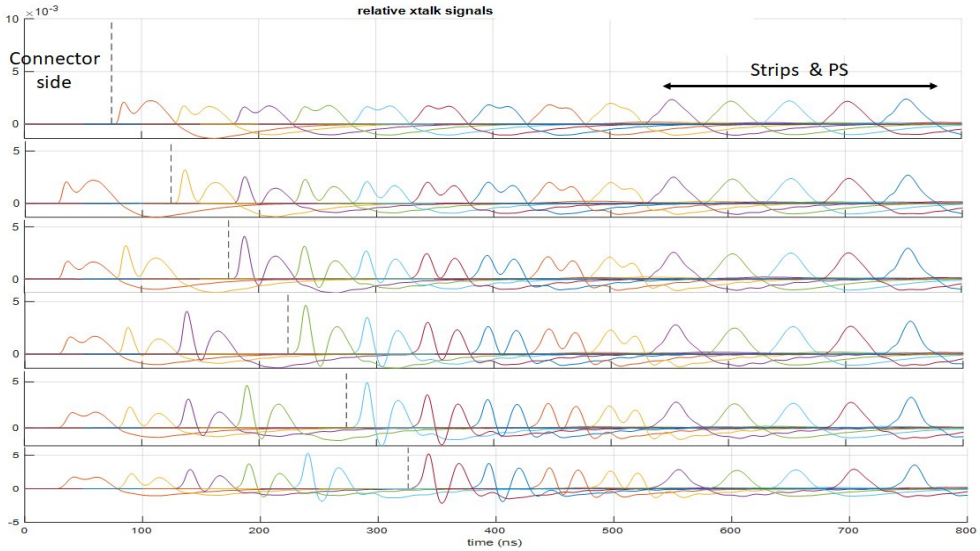

Figure 19: Measurement of all crosstalk signals (plotted sequentially from channel 1 to 15) for signal injection from channels 1 to 6. The dashed line shows the injection cell position . The shaping time is 20 ns.

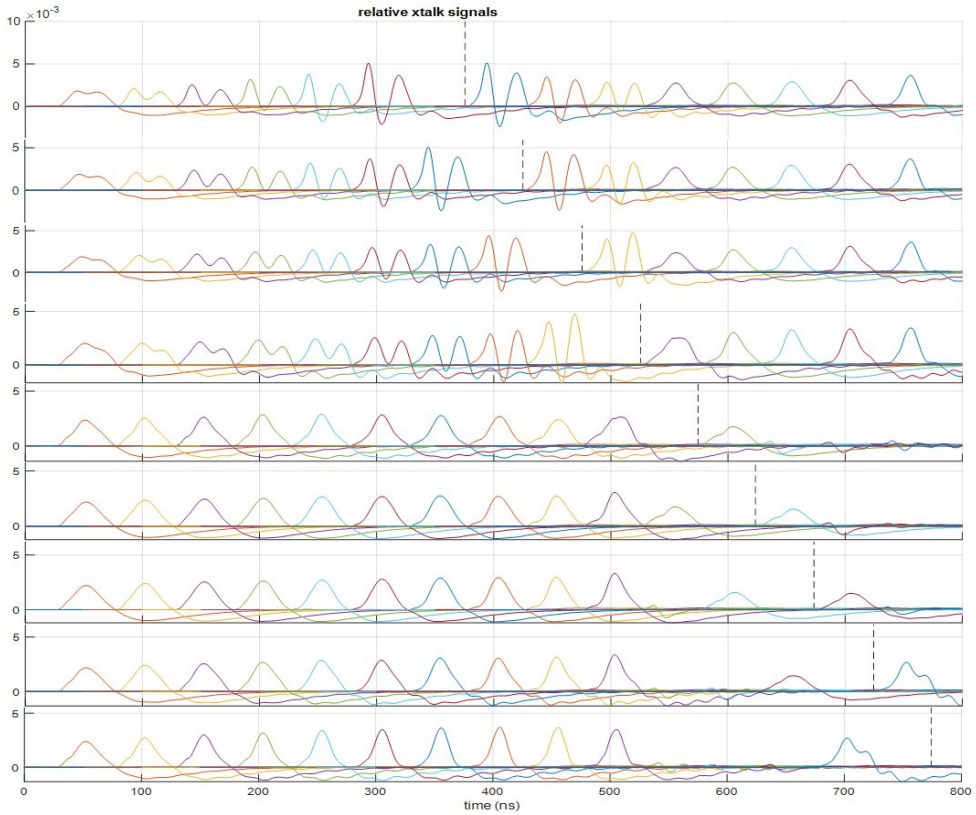

Figure 20: Measurement of all crosstalk signals (plotted sequentially from channel 1 to 15) for signal injection from channels 7 to 15. The dashed line shows the injection cell position. The shaping time is 20 ns

These measurements are qualitatively reproduced by simulation, using Cadence Sigrity to extract a behavioral model of the tower 3 of the PCB board (Cadence Sigrity produces a black box model, including thousand of basic passive components, which are tuned to fit as best as possible its electromagnetic simulation of the PCB) and LT-Spice to make the simulation of this extracted model in the time domain, as shown in figure 21:

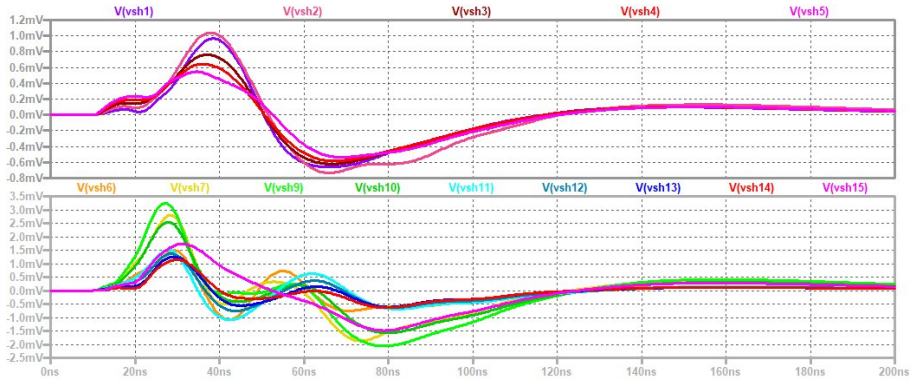

Figure 21: LT-Spice simulation of the model of the tower 3 of the PCB, extracted by Cadence Sigrity with 20ns shaping time, when a signal is injected on the cell 8. Top curves are for presampler and strips measurements and bottom curves are for all other cells.

From these waveforms (measured on figures 19 and 20 and simulated on figure 21), one can make three observations:

- The presampler and strip cells induce and are sensitive to capacitive coupling only. This is related to their low pad to ground capacitance (thus high impedance) implying that a reduced current flows in the pad to connector loop.
- All other cells exhibit both capacitive and inductive crosstalk
- Closer cells are more subject to inductive crosstalk than further cells.

A more basic model, shown in the appendix, leads to results similar to those obtained with Cadence Sigrity and reported in figure 21.

If one cross-checks the inductive crosstalk measurement with the capacitance measurement shown in figure 11, it seems the inductive part of the crosstalk is directly related to the pad-shielding part of the measured capacitance. This observation is confirmed by a measurement of tower 2 including some lateral shielding which increases this pad-shielding capacitance without changing the lineic capacitance:

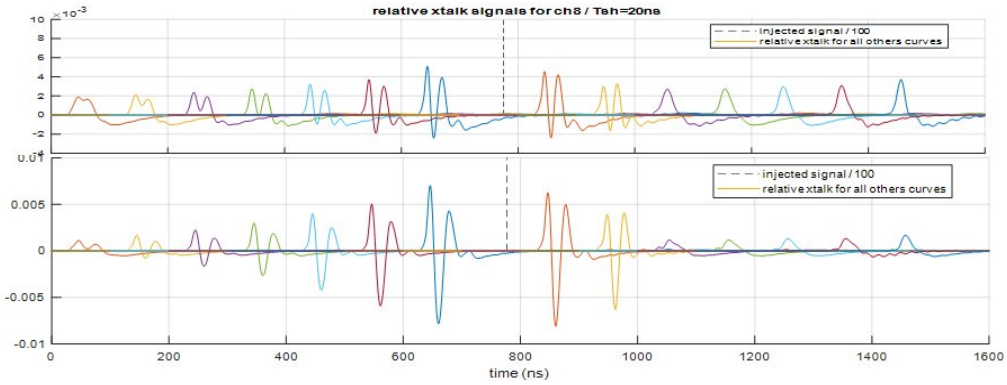

Figure 22: Comparison of crosstalk on tower 3, without lateral shielding (top) with crosstalk on tower 2, with lateral shielding (bottom). In both cases the direct signal, after shaping, has a peak amplitude of 1V. The shaping time is 20 ns.

In figure 22, both top and bottom images have the same scale. On the bottom image, with the extra lateral shielding, the crosstalk signals with capacitive effect only (i.e those of the strips and PS cells) are smaller than the ones on the top image, because of the better shielding between traces, but the crosstalk signals with an additional inductive effect exhibit larger signals because of the larger pad-shielding capacitance (13pF/trace without extra shielding and 21pF/trace with the extra shielding).

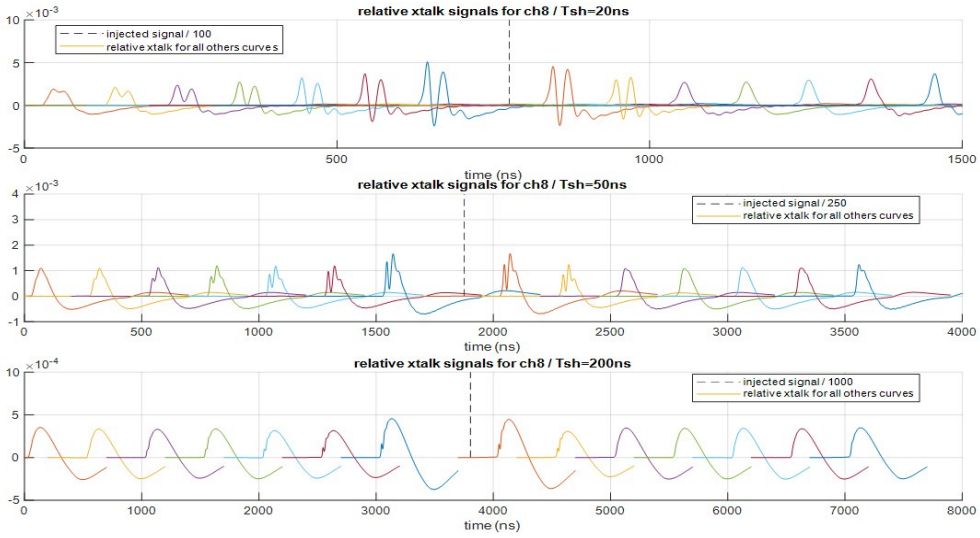

Figure 23: Effect of the shaping time on crosstalk signals. Shaping time = 20ns (top curve), 50ns (middle curve), 200ns (bottom curve) . In all cases the normalization is such that the direct signal, after shaping has a peak amplitude of 1V.

In figure 23, the increase of the shaping time reduces the crosstalk magnitude and attenuates at the same time the inductive effect which is faster than the capacitive effect and thus, more sensitive to the shaping time constant.

From these measurements, one can extract the maximum crosstalk ratio (peak of the cross-talk divided by peak of the direct signal) for each trace in both cases with (tower 2) or without (tower 3) additional lateral shielding, for different shaping times:

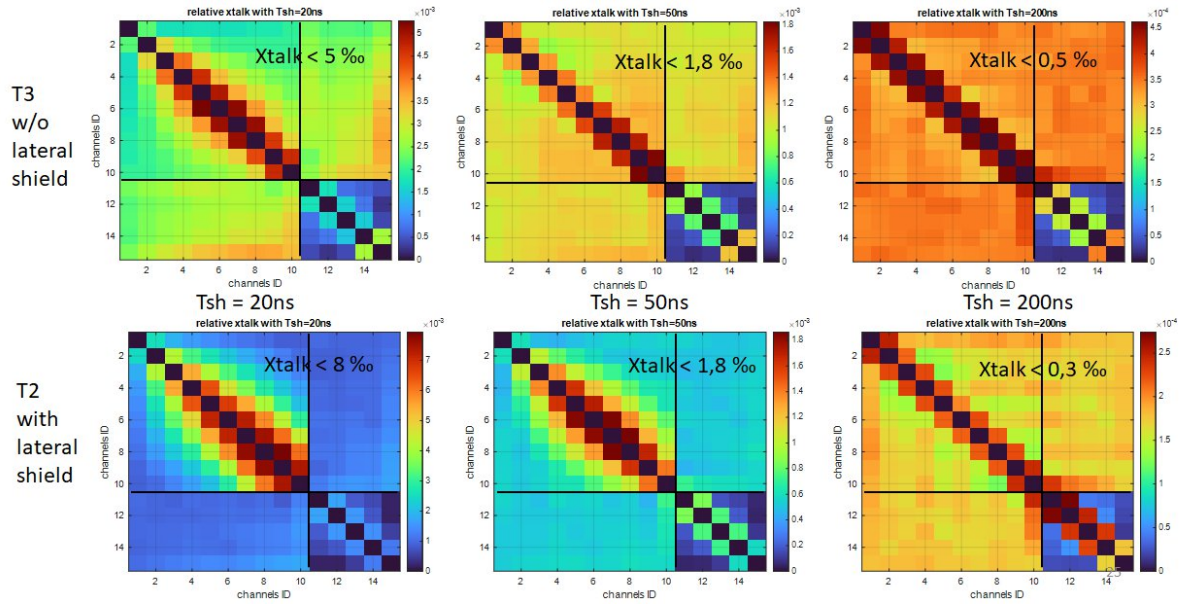

Figure 24: Maximum crosstalk ratio for towers 2 and 3, depending on the shaping time (20-50-200ns)

With or without lateral shielding, figure 24 shows a reduced crosstalk ratio when the shaping time is increased, because of the integration effect. But adding some lateral shielding does not reduce the total maximal crosstalk if the shaping time is faster than 50ns because of the inductive effect which is increased by the additional pad-shielding capacitance. The positive impact of the lateral shielding on the crosstalk ratio is effective only if a sufficiently large shaping time is used to reduce and almost cancel the fast crosstalk signal coming from the inductive effect.

The electrodes included in the electromagnetic calorimeter will be separated by large absorbers [1], connected to ground, which will play also the role of current return, in parallel with the shielding ground of the traces. To roughly mimic this effect, we placed an effective ground return, simulating an absorber, by putting a copper sheet on top of the PCB and connecting it to ground (see picture 25).

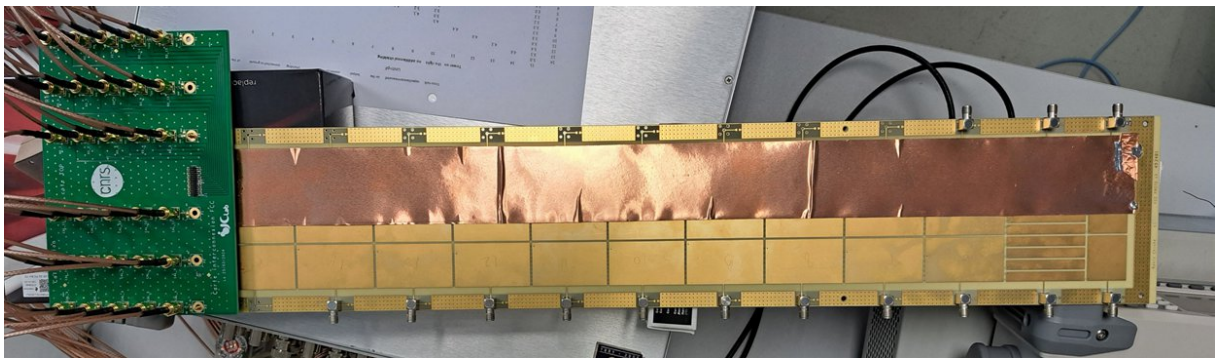

Figure 25: Picture of the pseudo-absorber made of a copper sheet soldered to ground, on top of the tower 3.

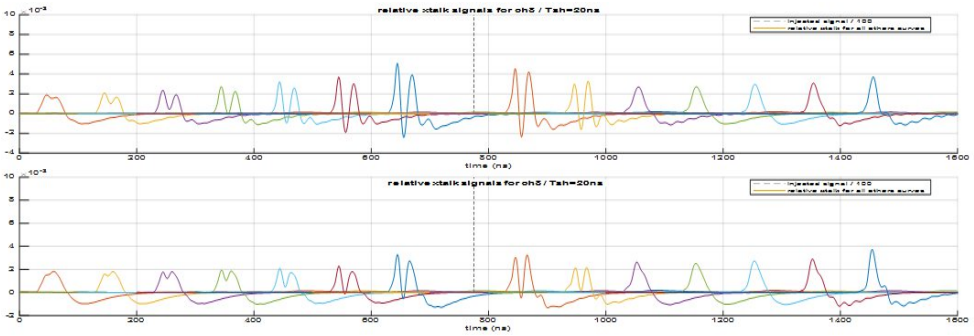

Figure 26: Crosstalk signals without the additional absorber sheet (top) and with the additional absorber sheet (bottom) . The shaping time is 20 ns.

Adding the pseudo-absorber does not change the capacitive crosstalk, as seen in particular on the last cells measurements (presampler and strips), but reduces the inductive crosstalk by stealing some current return from the shielding ground and returning it from the absorber ground.

As already shown in figure 24, one can work on the shaping time to reduce the crosstalk. In figure 27 plots, the shaping time is applied offline by numerical filtering on the measured data.While the cross-talk signals differ widely in amplitude and shape with a 20ns shaping, they become more similar when the shaping time is increased, mainly because the inductive cross-talk is progressively integrated out.

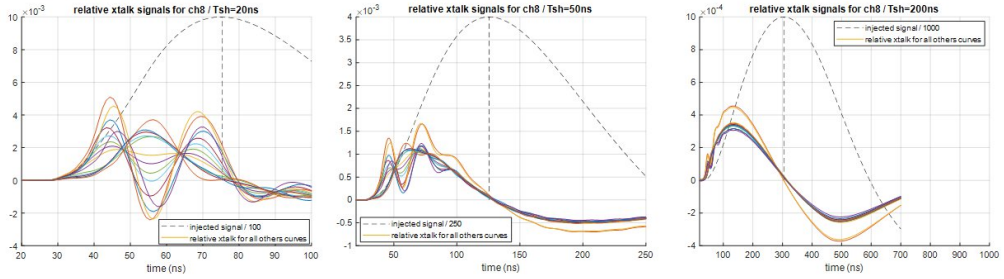

Figure 27: From left to right, measurement of the 14 crosstalk signals when the injection signal is connected to the 8th cell for 20ns, 50ns and 200ns.

As a summary, table-1 shows for the three shaping conditions the maximum of the cross-talk,and the cross-talk at the maximum of the direct signal when injecting on cell 8 of tower 3 of the PCB and table-2, the same measurements when injecting on any cell of the tower 3.

	20 ns	50 ns	200 ns
Maximum Xtalk (‰)	4.5	1.5	0.43
Xtalk at maximum of direct signal (‰)	2.5	0.16	0.04

Table-1: Maximum cross-talk and Cross-talk at the maximum of the direct signal, when injecting on cell 8 of tower 3, for different shaping values.

	20 ns	50 ns	200 ns
Maximum Xtalk (‰)	5	1.8	0.5

Table-2 Maximum cross-talk when injecting on any cell of tower 3, for different shaping values.

Summary:

- The choice of doubling the internal signal traces for symmetrizing the layers stacking changed the electromagnetic behavior of the lines. We have shown this type of line is properly described by the "differential stripline working in common mode" model. The result is a doubling lineic capacitance relatively to single internal traces and a lower characteristic impedance. The increase of the capacitance implies more electronic noise and is thus not a promising path for the future. This means we have to find a good way to produce a PCB with an asymmetric layer structure, although this is not recommended by manufacturers.
- We measured both capacitive and inductive crosstalk signals on the PCB. We found out the magnitude of the capacitive crosstalk can be reduced by adding some lateral shielding, at the expense of a larger pad capacitance. Such a lateral shielding also increases the inductive crosstalk as a consequence of the pad-shielding capacitance increase.
- We showed that a shaping time above 50ns reduces the magnitude of the inductive coupling to a negligible level.
- In the final calorimeter, it is envisaged to group by 2, or perhaps 4, neighboring cells from adjacent electrodes in azimuth, in order to limit the number of electronic channels. The setup described here allows to make measurements with 2 cells in parallel. Results will be reported in a future note.

We have benefited from discussions with M. Aleksa, B. François and J. Pekkanen, and from the help of C. Sylvia, A. Saussac, G. Ferry

References

[1] M.Aleksa et al "Calorimetry at FCC-ee" In: Eur. Phys. J. Plus 136.10 (2021) p.1066. DOI:10.1140/epjp/s13360-021-02034-2. and arXiv: 2109.00391 [hep-ex]

Appendix: How to build a basic behavioral model for the IJCLab PCB?

As opposed to the way followed to produce figure 21, based on an electromagnetic simulation, one can build a simple behavioral model based on our understanding of the PCB and on some simple measurements.

As seen in figures 5 to 8, a tower is made of 15 contiguous channels, separated in the z direction by a minimum distance of 1,27 millimeters center-to-center and each of these channels is made of a stripline of variable length, followed by a pad. In most cases (except for the presampler and for 3 of the 4 strips) some shieldings are underneath the pad region.

In the striplines, the distance between the signal trace and the shieldings (100 µm) is much smaller than the center-to-center distance between striplines. Thus, one can consider that the electric and the magnetic fields are properly confined inside the stripline and there is no crosstalk coupling in this region. A simple line model is sufficient to describe the stripline part.

Figure 28: Typical simulation schematic when injecting on channel 8. Crosstalk capacitances have only been set for channels in connection with channel 8.

For the channel 'n', the line behavior (characteristic impedance and delay) is:

$$Z_c(n) \simeq 29\Omega$$

$$\tau_d(n) \simeq \begin{cases} 100\,ps + (n-1).480\,ps & 1 \le n \le 10 \\ 4.9ns & 11 \le n \le 14 \\ 5.4ns & n = 15 \end{cases}$$

These values are similar to those found using equation 3.

Following the stripline is the region of the pad. As the measurements are made with a minimum shaping time of 20ns, the delay of this part can be neglected and the model considered will be the equivalent lump elements Lpad and Cpad. Cpad has been fitted in figure 11.

$$C_{pad}(n) \simeq \begin{cases} (15-n).13pF & 1 \le n \le 10 \\ 13pF & n = 11 \\ 0pF & 12 \le n \le 15 \end{cases}$$

The inductive part Lpad (which is mainly due to mutual induction) is difficult to measure and will be adjusted to produce a simulation result close to the measurements. The crosstalk capacitances between channels have been measured in tower 3 (see figure 13) around 3pF for all channels except for close neighbors (~ 5pF).

To properly simulate the inductive crosstalk, each mutual inductance was manually adjusted to progressively smaller values (30nH to 1nH) as the distance from the injection path increases.

Using these values one obtains the set of simulated crosstalk signals reported in figure 29. The agreement with figure 21 (simulation based on Cadence Sigrity) and figures 19 and 20 is considered good enough to validate the simplified model.

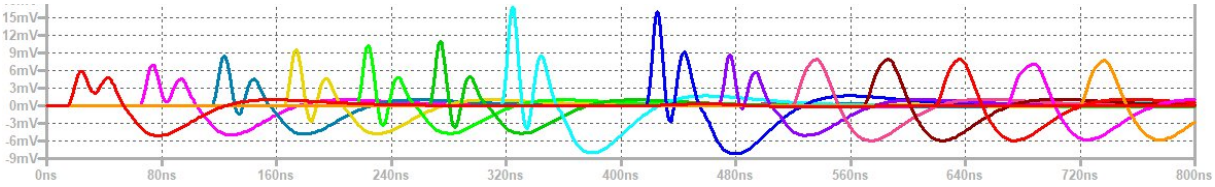

Figure 29: Typical crosstalk simulation results when injecting on channel 8. The different colors are related to channels 1 to 15.